

Electroplated Cu/Ni Coil Sensors for Cryogenic Applications: Low-Cost Temperature Monitoring in Industrial and Scientific Settings

Moh. Toifur^{1, a)}, Siti Zahra Helmania Putri¹, and Okimustava, and Eko Susanto¹

¹*Department of Physics Education Ahmad Dahlan University Yogyakarta, Indonesia*

^{a)} Corresponding author: toifur@mpfis.uad.ac.id

Abstract. Cryogenic temperature sensors are crucial in various scientific and industrial applications requiring precise low-temperature measurements, including in medicine, food technology, aerospace, and quantum research. This study presents the development of a low-cost temperature sensor using copper-nickel (Cu/Ni) wire fabricated through electroplating at different electrode voltages: 0 V, 4.5 V, 6.0 V, and 7.5 V. The electroplating process employed a $\text{NiSO}_4\text{-NiCl}_2\text{-H}_3\text{BO}_3$ electrolyte solution at 60 °C. The sensors were tested in liquid nitrogen to evaluate their performance in the cryogenic range, focusing on response time, voltage range, sensitivity, and hysteresis loss. All sensors demonstrated responsiveness within -160 °C to 0 °C . While the pure copper sensor showed the fastest response and widest voltage range (180 s and 0.02 V), it lacked thermal stability. The sensor plated at 4.5 V had a slower response (300 s) and moderate sensitivity, whereas increasing the deposition voltage to 6.0 V enhanced sensitivity and reduced hysteresis loss (0.0023 V), indicating improved stability. Comparisons with Ag, Cu, and Pt-100 sensors confirmed that Cu/Ni sensors, especially those deposited at 4.5 V and 6.0 V, provided significantly smaller resistance changes, highlighting their potential for stable and economical cryogenic temperature monitoring.

INTRODUCTION

Cryogenic temperature sensors are utilized across various sectors, particularly in food technology, enabling the rapid freezing of food products. This technique preserves the texture and quality of the food while significantly extending its shelf life [1]. Similar applications are found in preserving biological products or additives, such as probiotics and livestock semen [2].

In the medical field, cryogenic sensors are integral to technologies like Magnetic Resonance Imaging (MRI), which uses liquid helium to cool superconducting magnets [3]. Cryogenic treatment is also employed for tissue freezing in therapeutic applications. In industrial settings, especially the gas industry, these sensors are crucial for measuring the temperature in storage tanks of liquefied gases, including during transportation [4]. In biological research, cryogenic sensors help maintain optimal temperatures for storing cells, tissues, or organs [5].

In the aerospace sector, cryogenic temperature control is essential for managing components that operate in extremely low-temperature environments [6]. Similarly, in laboratory research, cryogenic sensors play a critical role in experiments sensitive to temperature fluctuations, such as those involving superconductivity, particle physics, and quantum research [7]. Materials used for low-temperature sensors must exhibit thermal stability, good electrical conductivity, and a responsive change in resistance or voltage with temperature variation. Common materials for temperature sensors include platinum (Pt), copper (Cu), nickel (Ni), constantan, specialized metal alloys such as germanium and Cernox, as well as semiconductors like glass diodes, silicon, and superconducting materials [8].

Nickel is highly suitable for low-temperature sensors due to its high temperature coefficient of Resistance (TCR), reaching up to $0.00672/\text{°C}$. It is cost-effective, easy to fabricate in various forms such as wires, thin films, or spirals, and offers precision at temperatures below 300 K [9]. Also, nickel is resistant to corrosion and oxidation at low temperatures and enables temperature reading without requiring complex electronic systems [10]. Nickel-coated

copper (Cu/Ni) wire exhibits excellent flexibility, allowing it to be coiled and facilitating assembly and integration with other electronic components [11]. At the interface between copper and nickel, a strong bond is formed due to the similar atomic sizes of the two materials, with nickel having a radius of 121 pm, slightly smaller than copper's 138 pm [11].

Mechanically, Cu/Ni wire demonstrates increased pliability, reducing the likelihood of damage [12]. As a temperature sensor, Cu/Ni wire is particularly suitable for measuring temperatures at specific points or localized areas (IST AG, n.d.). However, its wire form results in a smaller contact cross-sectional area. Additionally, the higher thermal mass of Cu/Ni wire leads to a slower response time. To address this, the number of coil turns should be increased, and the diameter should be reduced [13].

Electroplating is a more feasible and low-cost method for fabricating nickel-coated copper (Cu/Ni) wire due to its low operational cost, high quality, simple equipment requirements, and the ability to produce high-quality coatings. This technique suits complex geometries, such as wires and coils, requiring uniform and adherent metal layers.

Although previous studies have focused on the use of various materials for low-temperature sensors, such as Pt, Cu, Ni, and constantan, there is still a notable lack of research that deeply explores the use of copper-nickel (Cu/Ni) wire, particularly for cryogenic temperature sensors. Moreover, although nickel is well known for its high-temperature Coefficient of Resistance (TCR), the effect of deposition voltage variation during the electroplating process on sensor performance at cryogenic temperatures remains unclear. This study addresses this gap by investigating how variations in electrode voltage (0–7.5 V) influence response time, voltage range, sensitivity, and hysteresis loss at cryogenic temperatures, thus providing a more comprehensive understanding of the potential of Cu/Ni as an alternative material for cryogenic temperature sensors [14].

The development of Cu/Ni wire-based cryogenic temperature sensors contributes to the Sustainable Development Goals (SDGs) by improving equitable access to advanced medical technologies (SDG 3: Good Health and Well-being), fostering innovation and industrial development through the utilization of locally available resources (SDG 9: Industry, Innovation, and Infrastructure), and supporting sustainable and responsible production systems (SDG 12: Responsible Consumption and Production). Besides that, this sensor provides a low-cost alternative and can be flexibly designed for various applications.

In the context of vocational education, the electroplating topic and the application of cryogenic temperature sensors are highly relevant, as they provide practical skills that are in high demand in the engineering and manufacturing industries, particularly in the fields of materials science and sensor technology [1], [2]. By imparting knowledge and skills in electroplating and cryogenic temperature sensors, vocational education can prepare the younger generation to contribute to the rapidly growing industrial sector while enhancing domestic research and technological capacity [3].

RESEARCH METHODS

Experimental Procedure

The experimental procedure was conducted according to the scheme presented in Fig. 1.

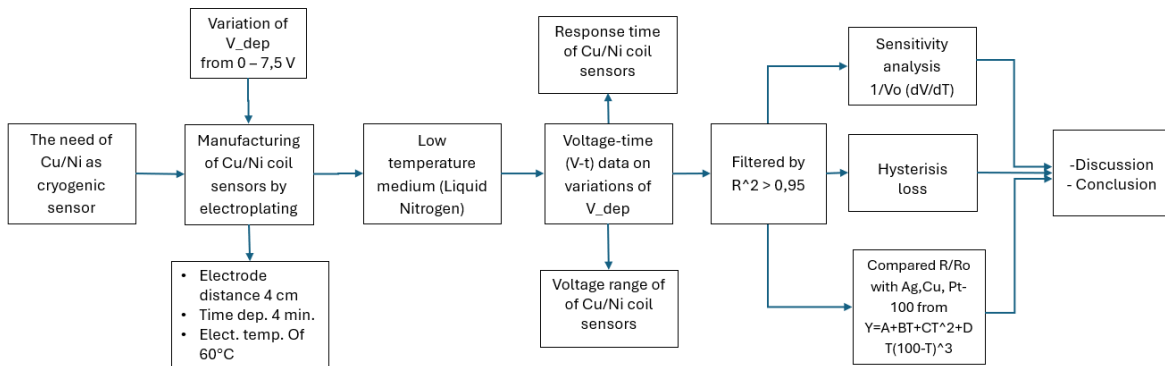


FIGURE 1. The experimental procedure employed in this research

Material Preparation

The initial step involves preparing materials such as copper wire coils, nickel plates, and an electrolyte solution consisting of NiSO₄ (260 g), NiCl₂ (60 g), H₃BO₃ (40 g), and deionized water (1000 mL).

Substrat Preparation

In the substrate preparation phase, the surfaces of the 0.5 mm copper wire and 10×1.5×0.01 cm³ nickel plate were meticulously cleaned by rubbing them with a soft cloth impregnated with Autosol SM583 metal polish. Polishing continued with a soft cloth coated with toothpaste until the surfaces appeared shiny. Subsequently, the copper wire and nickel plate were washed with Sunlight detergent, rinsed with deionized water, and cleaned with 95% alcohol in an ultrasonic cleaner for 3 minutes. After drying, the copper wire was weighed using an Ohaus PR223/E balance [15].

Fabrication of Cu/Ni Wire Sample

To prepare the Cu/Ni wire samples, an electroplating reactor was utilized. The copper wire was coiled into a 5 mm diameter coil with 100 turns. The coil was placed at the cathode, 4 cm away from the nickel plate, which served as the anode. Both electrodes were immersed in an electrolyte composed of NiSO₄ (260 g), NiCl₂ (60 g), H₃BO₃ (40 g), and deionized water (150 mL) at a temperature of 60°C. Electroplating was performed at a voltage of 4.5 V for 4 minutes. During the electroplating process, the current was measured using a DCP-BTA vernier. This process was repeated for other substrates at electrode voltages of 6.0 V and 7.5 V. The applied voltage during electroplating was selected in the range of 4.5–7.5 V to ensure uniform deposition and minimize defects on film. Lower voltages resulted in slow growth, whereas higher voltages led to rough and porous layers. The chosen range provided an optimal balance between deposition rate and surface quality, which is critical for cryogenic sensor performance. After electroplating, the samples were removed, cleaned with deionized water in an ultrasonic cleaner for 3 minutes, and dried using a hair dryer [16].

Data Acquisition

To obtain the response data of the Cu/Ni coil sample as a temperature sensor, the sample was gradually lowered into a liquid nitrogen Dewar flask together with a TCA-BTA thermocouple at a rate of 7 cm/min, with a sampling rate of one sample per second, until reaching the minimum temperature measurable by the thermocouple (approximately –165 °C). Subsequently, the sample was raised back to its original position. The sample response, in the form of voltage at both ends of the sample, was measured using a VP-BTA voltage sensor, while the thermocouple response was recorded as temperature. The data were processed using a LabQuest Mini transducer and displayed on a computer screen with Logger Pro™ 3 software in numerical, graphical, and various data processing and graphing formats [17].

Data Analysis

The numerical voltage data at different times (V_i , t_i) and for different deposition voltages are crucial for developing electroplated material-based sensors. These data were used to determine sensor quality and the influence of the material's microscopic structure on sensor performance, including voltage range, sensitivity, and hysteresis losses. The R/R0 value of the sample was compared with that of the Pt-100 sensor to assess the performance of a commercial sensor.

The voltage range was obtained by calculating the difference between the sensor voltage at the maximum and minimum temperatures:

$$\Delta V = V_{\max} - V_{\min} \quad (1)$$

For sensitivity, the semi-relative sensitivity to V_0 or the sensor voltage at 0°C was used [18], [19]:

$$S_T^V = \frac{1}{V_0} \frac{dV}{dT} \quad (2)$$

Hysteresis loss was determined by calculating the maximum voltage difference between the heating and cooling curves at the same temperature [20], [21]:

$$HL = (V_c - V_h)_{\max} \quad (3)$$

where HL , V_c , and V_h represent hysteresis loss, cooling voltage, and heating voltage, respectively.

To compare the temperature sensor performance with the Pt-100 sensor, the Callender-Van Dusen equation was used [22], [23]:

$$\frac{R}{R_0} = A + BT + C(T - 100)T^3 \quad (4)$$

where A, B, and C are constants. A determines the sensor sensitivity, B accounts for deviations from linearity, and C represents additional curve deviations. Ideally, A should be as large as possible, while B and C should be as small as possible. For the Pt-100 sensor, the constants are $A = 3.91E-03$, $B = -5.78E-07$, and $C = -4.18E-12$ [24], [25].

RESULTS AND DISCUSSION

Voltage – Time Curve

Figure 2 illustrates the voltage-time response of the Cu/Ni sensor when immersed in liquid nitrogen, transitioning from 0°C to approximately -160°C and subsequently warming back to 0°C. The characterization results demonstrate that Cu/Ni materials exhibit thermoresistive properties, where their electrical resistance varies with temperature. Deposition voltages of 0 V, 4.5 V, 6.0 V, and 7.5 V influence the sensor's output voltage levels but do not alter the general trend of the sensor's response to temperature changes [26]. The sensor's response to temperature variations is sufficiently sensitive and consistent, indicating the potential of Cu/Ni sensors for cryogenic temperature monitoring applications [27].

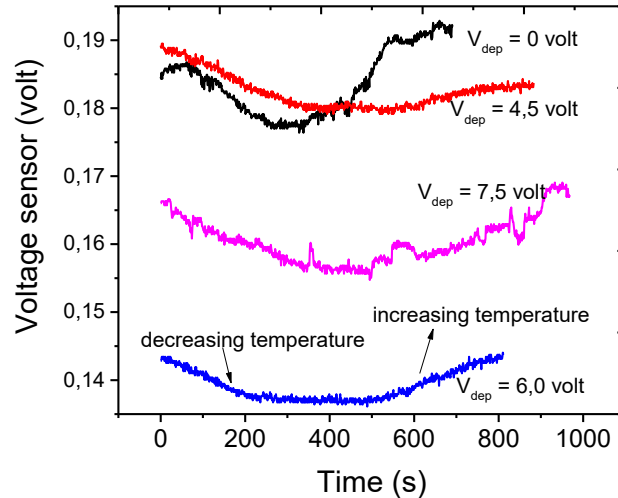


FIGURE 2. Voltage response of the Cu/Ni sensor during cooling and heating cycles in liquid nitrogen

Response Time

Subsequently, the output voltage of the Cu/Ni sensor ranged from 0.145 V to 0.195 V, depending on the deposition voltage, as appointed in Fig. 3. Uncoated Cu sensors were able to respond to temperature changes but lacked stability. Sensors electroplated at 6.0 V exhibited the lowest minimum voltage and stable signal characteristics, whereas those at 7.5 V showed voltage fluctuations [28]. The deposition voltage significantly affected the time required to reach the minimum voltage, as presented in Fig. 2. The pure Cu sensor (without Ni coating) exhibited the fastest response time of approximately 180 s. Cu/Ni sensors deposited at 4.5 V, 6.0 V, and 7.5 V required approximately 300 s, 350 s, and 310 s, respectively [27]. According to You et al., the increase in response time was attributed to the microscopic structure and surface morphology of the sensors, which introduced additional thermal barriers and reduced the heat transfer rate [26], [29].

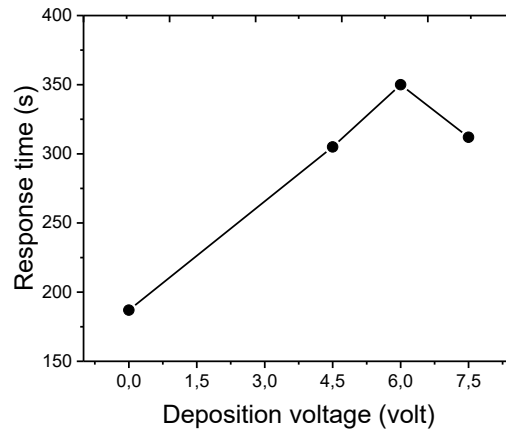


FIGURE 3. Response time of the Cu/Ni sensor during cooling from 0°C to -160°C

Voltage Range

The voltage range is crucial as it directly impacts the accuracy and overall performance of the system. If the sensor voltage is to be converted to an ADC, a wider voltage range leads to a higher resolution on the ADC, resulting in more accuracy. A good sensor has a voltage range close to the input voltage limit of the ADC, which is typically 0–5 V [30], [31].

Figure 4 indicates that the deposition voltage significantly affects the working voltage range of the Cu/Ni temperature sensor. The sensor deposited at $V_{dep} = 6.0V$ exhibited the smallest voltage range of 0.01 V, indicating a limited measurement capability. In contrast, sensors deposited at $V_{dep} = 0V$, 4.5 V, and 7.5 V showed wider voltage ranges, with the widest range of 0.02 V observed at $V_{dep} = 0V$. In electronic measurement systems, a small voltage range generally results in lower precision but offers greater signal stability due to minimal fluctuations. Conversely, a larger voltage range provides higher measurement accuracy but lower precision, as greater signal fluctuations reduce stability. Nevertheless, all observed voltage ranges and maximum output voltages remained within the detectable range of the ADC (1–5 V), although signal amplification of approximately 20 times was still required [32], [33].

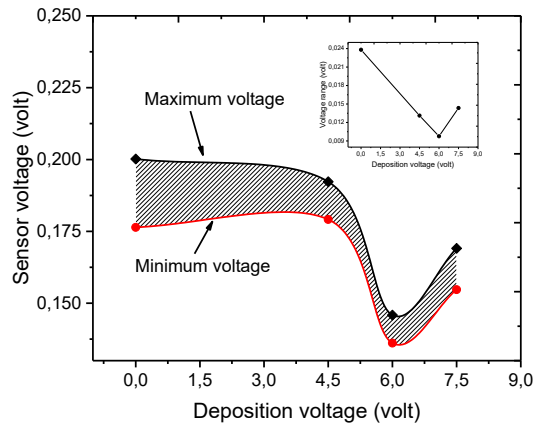


FIGURE 4. Characteristics of maximum and minimum sensor voltage and voltage range

Voltage-Temperature Curve

Figure 5 illustrates that, generally, all the curves show an increase in sensor voltage as the temperature rises, although with different slopes (sensitivities) depending on the deposition voltage.

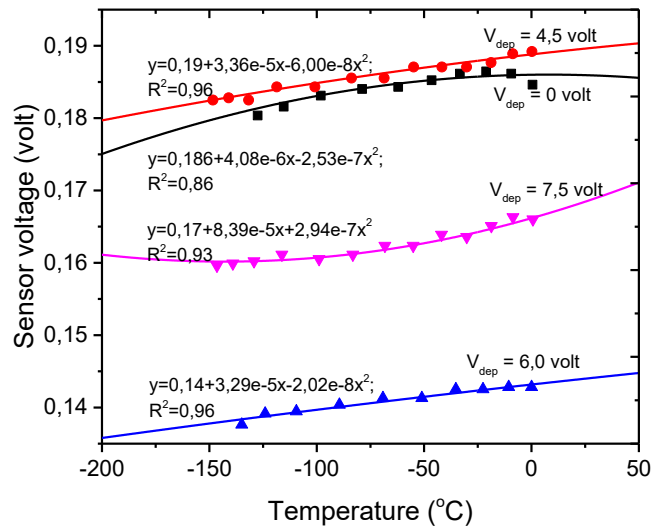


FIGURE 5. Voltage-temperature characteristics of Cu/Ni Coil sensors

The sensor fabricated with $V_{dep} = 4.5$ V exhibits the highest response to temperature changes. This is shown by the curve at the top of the graph and the highest gradient (slope) of the linear equation compared to the other sensors. Additionally, with the highest R^2 value (0.96), it indicates that the sensor's response to temperature changes is consistent, most stable, and highly accurate [28], [30].

On the other hand, the sensor fabricated at $V_{dep} = 0$ V shows reasonably good performance but still underperforms compared to the $V_{dep} = 4.5$ V sensor. This is likely due to the absence of a Ni layer, which could

enhance the sensor's surface response to temperature changes. This is further supported by the lowest $R^2 = 0.86$, suggesting that the data is more spread around the regression line. This indicates that the sensor could not consistently respond to temperature changes regarding the voltage output [31], [32].

The sensor output voltage tends to decrease at higher V_{dep} values of 6 V and 7.5 V. The curve for $V_{dep} = 6$ V even shows the lowest response to temperature changes, with the smallest sensor voltage across the entire temperature range. This decrease may be caused by forming a thick or rough Ni layer, which inhibits the conversion of temperature signals into voltage. However, the sensor still shows a high R^2 value of 0.96, indicating stable responses and high accuracy [33], [34]. For further analysis, only sensors with an R^2 value greater than 0.95 will be considered, as this indicates a significant influence of temperature on the sensor's voltage. Among the four sensors, two meet this criterion: the sensors with $V_{dep}=4.5$ V and $V_{dep}=6$ V.

Sensor Sensitivity

Figure 6 shows the sensitivity of two Cu/Ni coil sensors produced by electroplating at deposition voltages of 4.5 and 6.0 volts. Both sensors show a negative correlation between temperature and sensitivity: the lower the temperature, the higher the sensitivity.

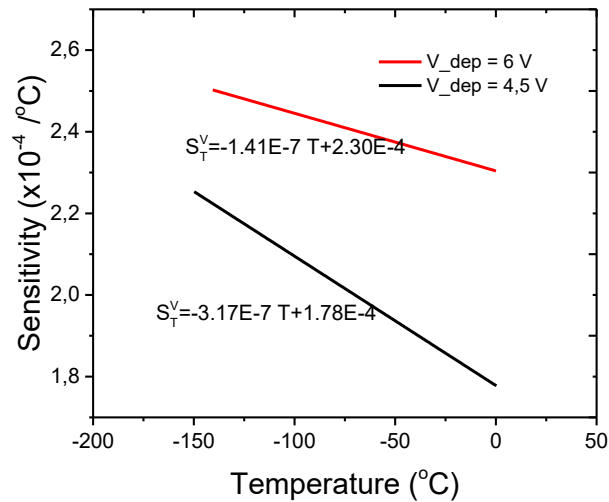


FIGURE 6. Sensitivity of two Cu/Ni coil sensors

The sensor with $V_{dep} = 4.5$ V has a steeper slope, meaning it is more sensitive to temperature changes compared to the sensor with $V_{dep} = 6.0$ V. At 0°C , the sensor with $V_{dep} = 6.0$ V exhibits higher sensitivity compared to the 4.5 V sensor. However, due to the sharper decrease in sensitivity at $V_{dep}=4.5$ V, the difference between the two sensors becomes smaller, or even reverses, at lower temperatures depending on the specific temperature appointed. Therefore, the 4.5 V sensor is more suitable for measuring dynamic temperatures, while the 6.0 V one is more appropriate for measuring stable temperatures [31], [35], [36].

Hysteresis Loss

Based on observations of the hysteresis loop area, as shown in Fig. 4, it can be concluded that the increase in electrode voltage during the sensor fabrication process affects the reduction of hysteresis losses. The sensor fabricated at $V_{dep} = 6.0$ V exhibited a smaller hysteresis loop area than the sensor at $V_{dep}=4.5$ V [37], [38].

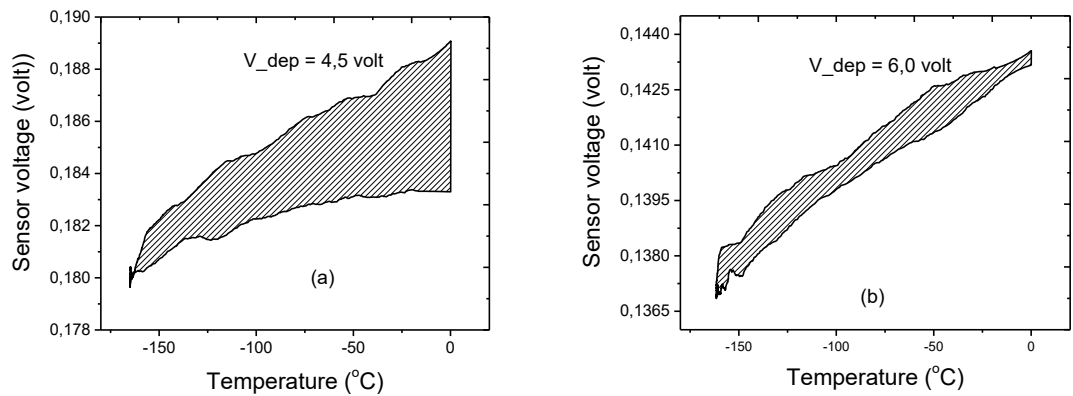


FIGURE 7. The hysteresis curve losses of two Cu/Ni coil sensors for calculating hysteresis losses. (a) $V_{dep}=4,5$ volt, (b) $V_{dep} = 6,0$ volt

For the $V_{dep} = 4.5V$ sensor, the hysteresis area appeared larger, with the sensor output voltage ranging from 0.1791 V to 0.1895 V and a large hysteresis loss of 0.0052 V. This indicates that, at the same temperature, the sensor voltage differs between the increasing temperature from $-160^{\circ}C$ to $0^{\circ}C$ and the reverse temperature. This leads to a larger voltage deviation [27,30]. In contrast, for the $V_{dep}=6.0V$ sensor, the hysteresis area was narrower, with a voltage range of 0.1355 V to 0.1445 V and a small hysteresis loss of 0.0023 V. This suggests that, at the same temperature, the sensor voltage was almost identical between the increasing temperature from $-160^{\circ}C$ to $0^{\circ}C$ and vice versa [31], [35]. This leads to a smaller voltage deviation [30].

Comparison of R/R_0 for Samples against Ag, Cu, and Pt-100

Figure 8 presents the data fitting results using Equation (4) for Cu/Ni coils fabricated at deposition voltages of 4.5 V and 6.0 V. For comparison, three reference materials - Ag, Cu, and Pt-100 - were included. The fitting constants obtained for each material are summarized in Table 1. These constants provide insight into the sensitivity and linearity of each material's response to temperature changes and highlight the performance differences between the electroplated Cu/Ni sensors and the reference materials.

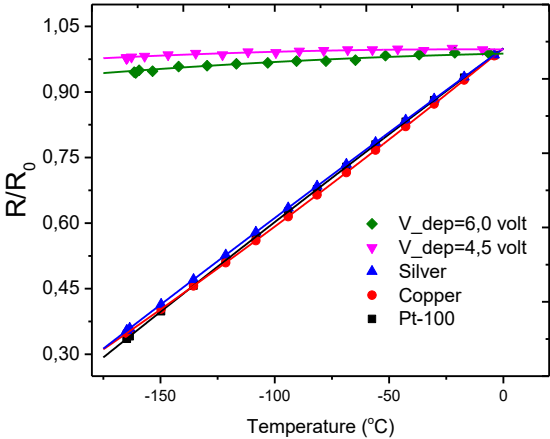


FIGURE 8. The comparison of R/R_0 between the two sensors of Cu/Ni coil and the reference materials Cu, Ag, and Pt-100

TABLE 1. Fitting constants for samples at $V_{dep} = 4.5$ V, 6.0 V, Silver, Gold, and Pt-100.

Parameter	$V_{dep} = 4,5$ V	$V_{dep} = 6,0$ V	Pt-100	Silver (Ag)	Gold (Au)
A	9,33E-05	5,99E-04	3,91E-3	3.821E-3	3.76E-3
B	4,11E-07	3,86E-06	-5,78E-07	-6.01E-7	-5.88E-7
C	-1,39E-11	-5,14E-11	-4,18E-12	very limited data	very limited data

The Silver, Copper, and Pt-100 sensors are highly sensitive and linear, as shown in Fig. 7, making it an ideal temperature reference standard. The sensor with $V_{dep} = 4.5$ V has a relatively flat curve, with R/R_0 values ranging from 0.95 to 1.01 throughout the temperature range. Compared to the three reference materials, the resistance change with temperature is minimal, which is $9.33E-5$ (from A constant), indicating lower sensitivity. The sensor with $V_{dep} = 6.0$ V also has a relatively flat curve, though slightly below the 4.5 V curve, with R/R_0 values ranging from 0.92 to 1.0. Compared to the three reference materials, the initial resistance slightly decreases as the voltage increases, and the temperature sensitivity remains low, which is $5.99E-04$ [39],[40]. Increasing the voltage (from 4.5 V to 6.0 V) does not significantly improve sensitivity compared to the three reference materials and even tends to reduce signal stability.

From the value of constant B, which determines the degree of deviation of the curve from its linear state as a measure of sensor stability, it is observed that the B value for the $V_{dep} 4.5$ V sensor is on the same order of magnitude as the B values of the three reference materials, that is 10^{-7} which is the smallest numerical value $4.11E-7$. Therefore, the sensor with $V_{dep} 4.5$ V is the most stable in responding to temperature changes compared to the others [40]. Meanwhile, the sensor with $V_{dep} 6.0$ V has the largest B value, $3.86E-6$, indicating that this sensor is unstable in responding to temperature changes [42].

Table 2 summarizes the analysis of the Cu/Ni sensors at $V_{dep} 4.5$ V and 6.0 V. The final column shows a comparison with standard materials, namely Ag, Cu, and Pt-100. Although the sensors have not yet reached optimal performance at low temperatures, this study provides valuable insight into their positioning relative to commercial sensors, allowing for improvements in future research.

TABLE 2. Performance characteristics of Cu/Ni sensors at different deposition voltages compared with Ag, Cu, and Pt-100.

Deposition Voltage	Response Time	Voltage Range	Temperature Response Consistency (R^2 of V-T Curve)	Sensitivity and Sensitivity Change	Hysteresis Loss	Comparison with R/R_0 of Ag, Cu, and Pt-100
0 V	Fast	Wide, with moderate noise	Poor	-	-	-
4.5 V	Moderately slow	Wide, slightly noisy	Excellent	High sensitivity, rapidly changing	Large, resulting in reduced accuracy	Less sensitive, most stable
6.0 V	Slow	Narrow, minimal noise	Good	High sensitivity, slowly changing	Small, resulting in higher accuracy	Less sensitive, less stable
7.5 V	Moderately slow	Wide, slightly noisy	Poor	-	-	-

CONCLUSION

1. The electroplating technique has been effectively utilized to coat copper wire with nickel at different electrode voltages (0–7.5 V), producing a Cu/Ni temperature sensor that reacts to changes in cryogenic temperatures.
2. The sensor with a 4.5 V electrode voltage exhibited the highest sensitivity to temperature changes with good linearity ($R^2 = 0.96$), making it suitable for high-temperature dynamic applications. Meanwhile, the 6.0 V electrode voltage sensor demonstrated the best signal stability with the lowest hysteresis loss (0.0023 V), making it more suitable for static and long-term temperature monitoring applications.
3. Although the performance of the Cu/Ni sensor has not yet matched the sensitivity of the commercial Ag, Cu, and Pt-100 sensors, the curve fitting results indicate that this sensor holds potential as a low-cost alternative with high design flexibility.
4. The development of Cu/Ni wire-based cryogenic temperature sensors will significantly impact various fields. In cryo-preservation, the sensor will enhance the accuracy of temperature monitoring. Similarly, LNG storage will improve the safety of LNG management and transportation. In aerospace, in controlling avionics systems.

ACKNOWLEDGMENT

The author would like to express sincere gratitude to LPPM-UAD for providing research funding under contract number: PT-038/SP3/LPPM-UAD/XI/2024.

REFERENCES

1. X. Ma, J. Li, L. Wang, and W. Zhang, *J. Food Technol.*, 2021.
2. X. Yin, M. Chen, F. Liu, and R. Zhao, *J. Biotechnol.*, 2021.
3. L. Deng, Q. Sun, J. Hu, and M. Wang, *J. Med. Eng.*, 2022.
4. A. Gupta and R. Pal, *J. Ind. Technol.*, 2023.
5. J. Zhou, H. Li, M. Xu, and Y. Chen, *Biotechnol. Adv.*, 2023.
6. S. Park, J. Kim, D. Lee, and S. Choi, *Aerosp. Sci. Technol.*, 2021.
7. H. Lee, M. Kang, S. Yoo, and J. Chung, *J. Phys. Mater. Sci.*, 2022.
8. M. Rahman, N. Ali, T. Hassan, and S. Ahmed, *Mater. Sci. J.*, 2021.
9. Y. Chen, L. Zhang, B. Wang, and C. Liu, *Mater. Res. Bull.*, 2023.
10. Z. Huang, F. Li, T. Yang, and H. Zhao, *J. Mater. Sci. Technol.*, 2022.
11. L. Zhang et al., *J. Appl. Phys.*, 2020.
12. AZoM, *AZoM Mater.*, 2017.
13. Nickel Institute, *Nickel Plating Handbook*, 2023, available at https://nickelinstitute.org/media/lxxh1zwr/2023-nickelplatinghandbooka5_printablepdf.pdf.
14. Haynes International, *A Guide to the Metallurgical, Corrosion, and Wear Characteristics*, 2022, available at <https://haynesintl.com/wp-content/uploads/2023/06/a-guide-to-the-metallurgical-corrosion-and-wear-characteristics>.
15. M. Taufiqurrahman, M. Toifur, O. Ishafit, Okimustafa, and A. Khusnani, *Int. J. Adv. Res. Eng. Technol.* **11**, 333 (2020).
16. ISO 7846:2014, *Temperature sensors - Resistance thermometers with industrial platinum resistance elements*, *Int. Organ. Stand.*, 2014.
17. L. Zhang, X. Li, and Y. Chen, *J. Mater. Sci. Technol.* **45**, 456 (2020).
18. L. Michalski, K. Eckersdorf, J. Kucharski, and J. McGhee, *Temperature Measurement*, 2nd ed. (John Wiley & Sons, New York, 2019).
19. M. R. Islam and C. E. Davis, *IEEE Sens. J.* **20**, 2503 (2020).
20. T. Velmurugan, T. Sakthivel, and S. Rajasekaran, *IEEE Sens. J.* **20**, 13772 (2020).

21. L. Wang, H. Wang, and X. Liu, *Sensors* **21**, 489 (2021).
22. H. Sanson, J. G. Webster, and A. G. Skafidas, *IEEE Sens. J.* **21**, 3470 (2021).
23. M. Kobayashi and T. Adachi, *Measurement* **148**, 106920 (2020).
24. F. M. P. Alper, *Int. J. Thermodyn.* **26**, 73 (2023).
25. S. Sarkar, *Cogent Eng.* **5**, 1558687 (2018).
26. D. Setiamukti, M. Toifur, O. Ishafit, and A. Khusnani, *Sci. Technol. Indones.* **5**, 28 (2020).
27. M. Toifur, R. N. Islamiyati, and A. Khusnani, *SPEKTRA J. Fis. Apl.* **9**, 1 (2024).
28. H. Johnson and R. Smith, *Int. J. Sens. Technol.* **16**, 112 (2022).
29. Y. You, B. Liang, S. Liu, X. Zhang, and H. Zhang, *Micromachines* **12**, 265 (2021).
30. A. Patel and Y. Choi, *J. Therm. Sci.* **35**, 672 (2023).
31. T. Brown and M. Green, *Sens. Actuators A Phys.* **287**, 102 (2029).
32. S. Kim, H. Park, and M. Lee, *J. Surf. Sci.* **72**, 121 (2029).
33. J. White and Z. Liu, *J. Appl. Phys.* **87**, 58 (2021).
34. P. Adams, F. Brown, and J. Lee, *Cryogen. Eng. J.* **63**, 100 (2023).
35. V. Kumar and P. Jain, *Mater. Sci. Eng. A* **118**, 248 (2023).
36. S. P. Patel and R. S. Gupta, *Mater. Sci. Eng. B* **273**, 52 (2022).
37. L. Zhang and J. Zhang, *Sens. Mater.* **31**, 1721 (2023).
38. F. Liu and Q. Wang, *Adv. Funct. Mater.* **46**, 2089 (2023).
39. H. Wang, X. Zhang, and L. Liu, *Sens. Actuators B Chem.* **364**, 131935 (2023).
40. J. White and Z. Liu, *Sens. Actuators A Phys.* **314**, 112290 (2022).
41. Y. Zhang, W. Li, and H. Zhou, *Sens. Actuators A Phys.* **316**, 112 (2021).
42. S. Yang, J. Zhang, and T. Lee, *Appl. Phys. Lett.* **120**, 051906 (2022).